Density Functional and MP2 Studies of Germylene Insertion into C−H, Si−H, N−H, P−H, O−H, S−H, F−H, and Cl−H Bonds

Ming-Der Su* and San-Yan Chu*

Department of Chemistry, National Tsing Hua University, Hsinchu 30043, Taiwan, R.O.C.

Received: May 19, 1999; In Final Form: August 10, 1999

The potential energy surfaces for the insertion reactions of germylene into XH_n molecules have been characterized in detail using ab initio molecular orbital theory and density functional theory. The model system $Ge(CH_3)_2 + XH_n$ (X = C, N, O, F, Si, P, S, and Cl; $n = 1-4$) has been chosen for the present study. All the interactions involve the initial formation of a donor−acceptor complex, followed by a high-energy transition state, and then an insertion product. The agreement between MP2 and B3LYP results indicates that the latter provides an adequate theoretical level for further investigations of molecular geometries, electronic structures, and kinetic features of the germylene reactions. The following conclusions emerge from this work: (i) the X−H insertion reactions of germylene occur in a concerted manner via a three-membered-ring transition state, and that the stereochemistry at the heteroatom X center is preserved; (ii) the stabilization energies of the germylene−XH_n complexes increase in the order $NH_3 > H_2O > PH_3 > H_2S \sim HF > HCl \gg SiH_4 \sim CH_4$; (iii) the order of reactivity for X−H bonds toward germylene insertion is Cl > F > S > O > P > N ≫ Si > C. In other words, the greater the atomic number of heteroatom (X) in a given row, the easier the insertion reaction of XH_n hydrides and the larger the exothermicity. Moreover, the present study demonstrates that both electronic and steric effects play a major role in the course of insertion reactions of germylene into X−H bonds. This work also indicates that the chemical behavior of germylene should be more similar to that of silylene than to that of carbene species.

I. Introduction

The considerable interest devoted to carbene chemistry, due to the importance of divalent carbon species in organic chemistry, has given rise to the development of the study of other divalent species of group 14.[1] Silylene chemistry is well-developed,[2] but the chemistry of germylenes remains rather limited,[3] mainly due to the low stability of these intermediates and to their strong tendency to polymerize.[4] Nevertheless, germylenes have received much attention in recent years, not only because of the growing use of organogermanium compounds in synthesis, but also because of the role they may play in a variety of semiconductor growth processes. In this regard, knowledge of the factors determining the germylene reaction is of fundamental importance in understanding, modeling, and improving mechanistic germanium chemistry.

In principle, the germylenes undergo the same type of reactions as the carbenes and silylenes—insertion and addition. In this work, we shall focus on the insertion chemistry of germylenes.[5] It has been reported that the free germylene, Me_2Ge, can insert into C−H, Si−H, N−H, O−H, and S−H bonds of various organic compounds to yield substituted organogermanium hydrides of the type $Me_2Ge(X)(H)$.[6,7] However, no detailed mechanistic studies of insertion reactions of germylenes into σ bonds have been performed so far. Indeed, it is very difficult to detect the intermediate and the transition state due to the limitations in current experimental techniques. Theory is therefore a potentially useful partner to experiment in the investigation of the mechanism of germylene insertion reactions.[8]

To examine the generality of the germylene insertion, we have now undertaken a systematic investigation of the insertion reactions of dimethylgermylene into first- and second-row hydrides XH_n (where X is a p-block element) using density functional theory (DFT).

$$Ge(CH_3)_2 + H-XH_{n-1} \rightarrow Ge(CH_3)_2(H)(XH_{n-1}) \quad (1)$$

$$X = C, Si, N, P, O, S, F, Cl$$

$$n = 4, 4, 3, 3, 2, 2, 1, 1$$

These reactions have been chosen because they represent various kinds of germylene insertions for which experimental results have been reported by several groups.[6,7] The reason for choosing the dimethylgermylene as the starting material is that, according to our previous study,[8] $Ge(CH_3)_2$ was found to have a low activation energy for C−H bond insertions. It is thus reasonable to predict that $Ge(CH_3)_2$ should also easily activate other X−H bonds of XH_n hydrides. Our principal aim in the present work is to assess the performance of DFT in describing germylene insertions. We also include for comparison results obtained using the Møller−Plesset perturbation theory. Furthermore, through this theoretical work, we hope (i) to clarify the reaction mechanism and to determine the structures and energetics of the intermediate complexes and transition states, (ii) to investigate the thermodynamics of the germylene insertion reactions with CH_4, SiH_4, NH_3, PH_3, H_2O, H_2S, HF, and HCl molecules, (iii) to estimate their activation barriers and to understand the origin of the barrier heights, (iv) to establish general trends and predictions for the insertion of germylene into H−X bonds, and (v) to compare the germylene insertion with the analogous carbene and silylene insertions.

10.1021/jp9916440 CCC: $18.00 © 1999 American Chemical Society
Published on Web 11/18/1999

TABLE 1: Relative Energies and Geometries of Divalent Species $A(CH_3)_2$ (A = C, Si, and Ge) Obtained Using the B3LYP/6-311G* Level of Theory

$A(CH_3)_2$	state	ΔE_{rel} (kcal/mol)	A−C (Å)	∠CAC (deg)
$C(CH_3)_2$	$^1A'$	0.0	1.473	112.3
$C(CH_3)_2$	$^3A''$	−0.6906	1.468	133.5
$Si(CH_3)_2$	$^1A'$	0.0	1.917	97.65
$Si(CH_3)_2$	$^3A''$	25.63	1.907	118.5
$Ge(CH_3)_2$	$^1A'$	0.0	2.017	95.51
$Ge(CH_3)_2$	$^3A''$	30.65	2.008	118.5

II. Theoretical Methods

All geometries were fully optimized without imposing any symmetry constraints, although in some instances the resulting structure showed various elements of symmetry. For our DFT calculations, we used the hybrid gradient-corrected exchange functional proposed by Becke,[9] combined with the gradient-corrected correlation functional of Lee, Yang, and Parr.[10] This functional is commonly known as B3LYP, and has been shown to be quite reliable for geometries.[11] A standardized 6-311G basis set[12] was used together with polarization (*) functions.[13] The structures were then reoptimized with the 6-311G* basis set at the second-order Møller−Plesset perturbation (MP2) level of theory[14] for comparison with the B3LYP results. Accordingly, all geometries were optimized at the B3LYP/6-311G* level for all the B3LYP calculations and at the MP2/6-311G* level for conventional ab initio calculations. The stationary points on the potential energy surface were characterized by calculations of vibrational frequencies at the B3LYP/6-311G* and MP2/6-311G* levels. All of the DFT and MP2 calculations were performed with the GAUSSIAN 94 package of programs.[15]

III. Results and Discussion

Before the presentation of the calculated results for those insertion reactions, it is perhaps worthwhile to recall briefly the electronic structure of germylene. It is well established that germylene has a relatively low-lying σ lone-pair orbital and a higher-lying π (p in Ge) orbital.[8,16] The dominant configuration of a singlet germylene is $\sigma^2\pi^0$, while that of a triplet is $\sigma^1\pi^1$. In Table 1 the DFT-calculated equilibrium geometries of the first two states of $Ge(CH_3)_2$ are compared with analogous DFT calculations for $C(CH_3)_2$ and $Si(CH_3)_2$.[17] It is apparent that there is a great difference between $C(CH_3)_2$ and $Si(CH_3)_2$, while only minor geometrical changes and small differences in singlet−triplet splittings occur between $Si(CH_3)_2$ and $Ge(CH_3)_2$. The fact that there is a great similarity between germylene and its silicon analogues strongly implies that the germylene species should behave more like silylene than carbene. We shall see the theoretical results confirm this prediction in a later section.

Since the ground state of $Ge(CH_3)_2$ is known to be a singlet and its calculated singlet−triplet gap is large (see Table 1),[8,16] only the singlet surface was considered throughout this work. The geometries of the critical structures in the present calculations at the B3LYP and MP2 levels of theory are shown in Figures 1 and 2 (the MP2 values are in parentheses). The relative reaction energies for the insertion reactions obtained at the same level of theory are collected in Table 2. Note that the prediction of geometric parameters seems to be consistent with changing the theory level of both ab initio and DFT methods. Morever, the relatively small change in geometry upon reoptimization with the MP2 wave function is reflected in the small changes in total and relative energies at those stationary points. Thus, unless otherwise noted, we shall use only the B3LYP results in the following discussion for the sake of convenience.

TABLE 2: Relative Energies for the Process $Ge(CH_3)_2$ + H−XH_{n-1} → Precursor Complex → Transition State → Insertion Product[a]

system[b]	reactant (kcal/mol)	ΔE_{bind}[c] (kcal/mol)	ΔE_{act}[d] (kcal/mol)	ΔH[e] (kcal/mol)
CH_4	0.0	−0.0157	+39.1	−25.1
	(0.0)	(−1.11)	(+35.6)	(−32.6)
NH_3	0.0	−20.8	+25.1	−33.3
	(0.0)	(25.0)	(+22.7)	(−40.4)
H_2O	0.0	−13.9	+14.8	−45.1
	(0.0)	(−16.2)	(+15.1)	(−50.2)
HF	0.0	−7.19	+4.74	−59.1
	(0.0)	(−7.07)	(+9.57)	(−61.2)
SiH_4	0.0	−0.582	+15.7	−33.8
	(0.0)	(2.15)	(+11.4)	(−41.3)
PH_3	0.0	−8.97	+11.7	−37.4
	(0.0)	(14.1)	(+8.11)	(−46.1)
H_2S	0.0	−6.11	+5.97	−45.8
	(0.0)	(9.74)	(+3.89)	(54.9)
HCl	0.0	−1.61	+1.20	−56.4
	(0.0)	(3.71)	(+2.51)	(−64.2)

[a] All were calculated at the B3LYP/6-311G* and MP2/6-311G* (in parentheses) levels of theory. [b] The stationary point structures; see Figures 1 and 2. [c] The binding energy of the precursor complex, relative to the corresponding reactants. [d] The activation energy of the transition state, relative to the corresponding reactants. [e] The exothermicity of the product, relative to the corresponding reactants.

A. Precursor Complexes. It is reasonable to expect that the first step in the germylene reaction with small molecules is the formation of a precursor complex (PC). The calculated geometries of the precursor complexes (CH_4-PC, SiH_4-PC, NH_3-PC, PH_4-PC, and H_2O-PC, H_2S-PC, HF-PC, HCl-PC) are depicted in Figures 1 and 2, respectively. The binding energies obtained at both B3LYP and MP2 levels are given in Figure 3 as a function of atomic number, and the binding energies of the XH_n hydrides are given in Table 2.

Several interesting conclusions can be drawn from these figures and the table. First, in the case of CH_4 and SiH_4, their precursor complexes (CH_4-PC and SiH_4-PC) all display similar Me_2Ge- - -XH_4 bonding characteristics. That is, the XH_4 molecule is coordinated to Ge in an η^2 fashion via one X−H σ bond with the Ge−X−H plane nearly orthogonal to the Ge-$(CH_3)_2$ coordination plane. Calculated vibrational frequencies for the precursor complexes show that these structures are true minima on the potential energy surface. The calculated Ge−X bond distance in CH_4-PC and SiH_4-PC is 4.54 and 3.75 Å, respectively, as shown in Figure 1. The Ge−X bond distances are exceptionally long, indicating very little, if any, energy stabilization by reactant complexation. The simplest explanation of such long bond distances is that it is a steric effect. It seems unlikely that the species exists in gas-phase germylene/methane or germylene/silane mixtures at room temperature because the stabilization energies of CH_4-PC and SiH_4-PC are 0.016 and 0.58 kcal/mol, respectively, which are too low. Indeed, to our knowledge, no experimental detection of germylene−alkane or germylene−silane complexes formed during the reaction has been reported yet.

The closed-shell germylene electron configuration is such that there is a vacant p orbital on Ge capable of forming chemical bonds with a Lewis base, such as ammonia, water, or hydrogen fluoride. As can be seen in Figures 1 and 2, those precursor complexes (NH_3-PC, PH_3-PC, H_2O-PC, H_2S-PC, HF-PC, and HCl-PC) appear to have the same structure, in which optimal overlap between the lone-pair orbital of XH_n (n = 1−3) and the empty p orbital of germylene is achieved by an orthogonal

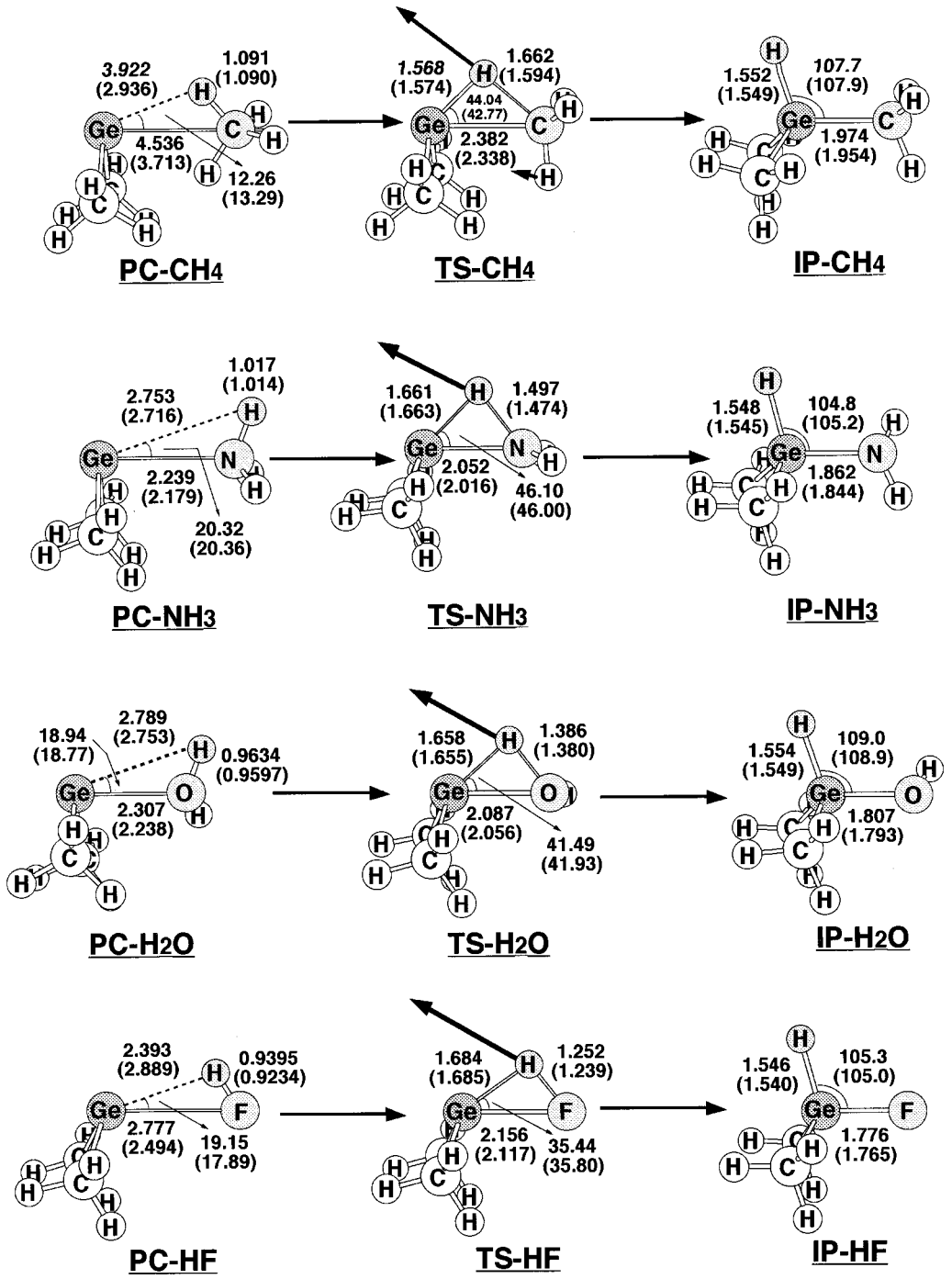

Figure 1. Optimized geometries (in Å and deg) for the precursor complexes (PC), transition states (TS), and insertion products (IP) of $Ge(CH_3)_2$ with the CH_4, NH_3, H_2O, and HF molecules. All were calculated at the B3LYP/6-311G* and MP2/6-311G* (in parentheses) levels of theory. The heavy arrows indicate the main atomic motions in the transition state eigenvector.

plane approach to the two molecules (see **1**). The donor−

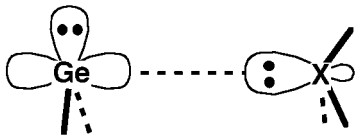

1

acceptor interaction leads to calculated Ge−N, Ge−P, Ge−O, Ge−S, Ge−F, and Ge−Cl bond distances of 2.24, 2.57, 2.31, 2.79, 2.78, and 3.18 Å, respectively, much shorter than those calculated for CH_4-PC and SiH_4-PC. Our attempt to locate the molecular complexes at much longer Ge−X distance for the addition of the dimethylgermylene to the XH_n ($n = 1-3$) molecules failed. Thus, our theoretical findings suggest that those complexes obtained in this work can be considered as Lewis acid−base adducts. As expected from the nature of the donor−acceptor complex, germylene should form much more stable complexes with those Lewis base molecules than with methane and silane. This prediction is confirmed by our theoretical results as given in Table 2. It is interesting to note that the stability of the intermediate complex is larger for XH_3 molecules than for XH_2 and XH molecules, and even larger than it is for XH_4 molecules. Namely, the stabilization energy

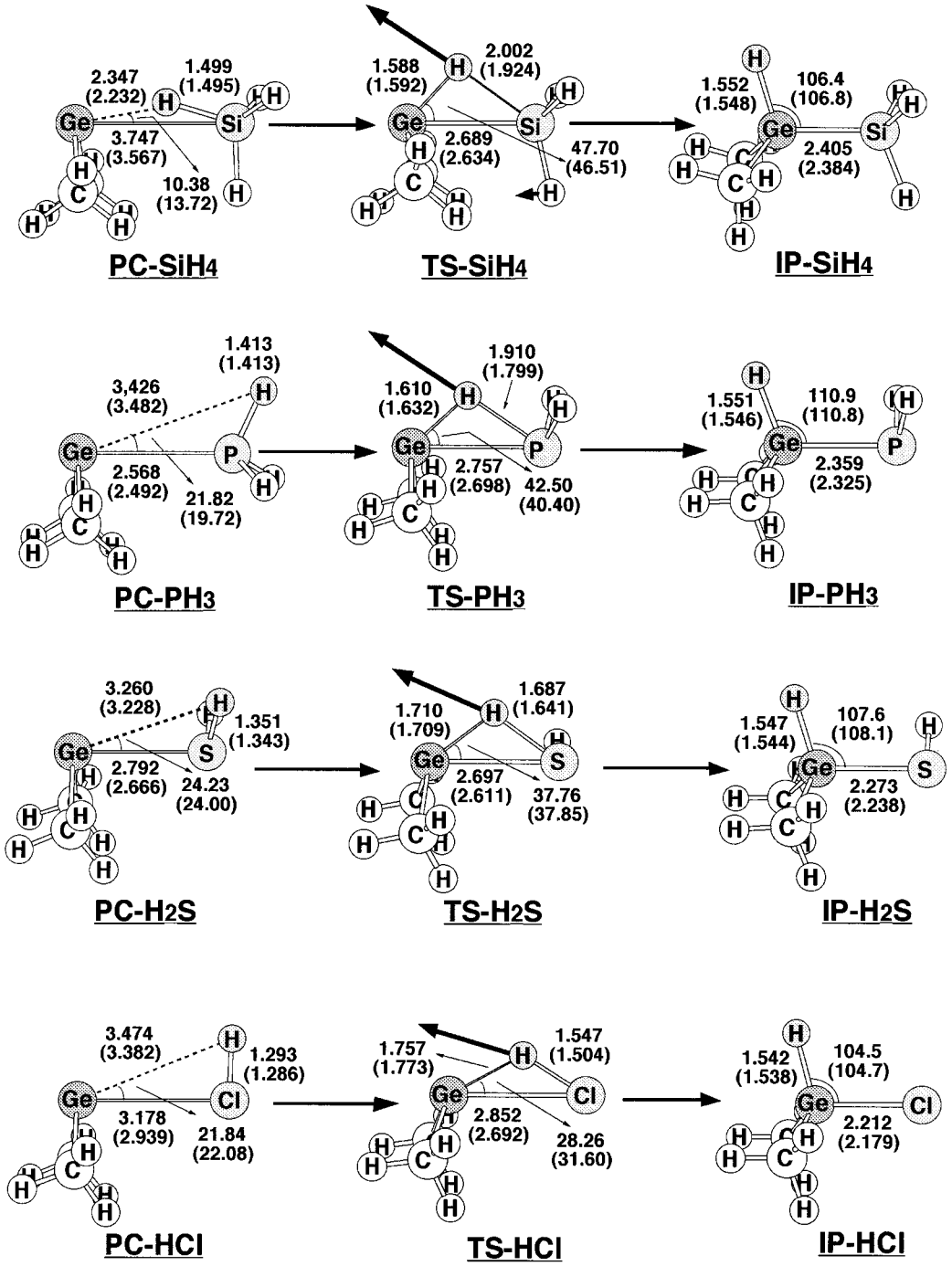

Figure 2. Optimized geometries (in Å and deg) for the precursor complexes (PC), transition states (TS), and insertion products (IP) of $Ge(CH_3)_2$ with the SiH_4, PH_3, H_2S, and HCl molecules. All were calculated at the B3LYP/6-311G* and MP2/6-311G* (in parentheses) levels of theory. The heavy arrows indicate the main atomic motions in the transition state eigenvector.

decreases in the order NH_3-PC (21 kcal/mol) > H_2O-PC (14 kcal/mol) > HF-PC (7.1 kcal/mol) > CH_4-PC (0.016 kcal/mol) and PH_3-PC (9.0 kcal/mol) > H_2S-PC(6.1 kcal/mol) > HCl-PC (1.6 kcal/mol) > SiH_4-PC (0.58 kcal/mol). The difference in stability of these adducts is easily understood in terms of the HOMO (Lewis base; i.e., XH_n)−LUMO (Lewis acid; i.e., dimethylgermylene) interaction.[18] According to the perturbation theory, both a smaller HOMO−LUMO gap and a larger overlap between them results in a greater Lewis adduct stabilization. According to our theoretical investigations, we note that the energy of the HOMO decreases in the order NH_3 > H_2O > HF and PH_3 > H_2S > HCl. On the other hand, the B3LYP results of Figures 1 and 2 show that the Ge−X bond distance increases in the order Ge−N (2.24 Å) < Ge−O (2.31 Å) < Ge−F (2.78 Å) and Ge−P (2.57 Å) < Ge−S (2.79 Å) < Ge−Cl (3.18 Å). Thus, the binding energy between $GeMe_2$ and XH_n increases as X varies from F to O to N and from Cl to S to P. In addition, there is a tendency for a reduction in interaction energies between the first and second row hydrides, which is mainly due to the increase of atomic radius of X going from the first- to second-row. This leads to a longer Ge−X distance and, in turn, a smaller overlap between the germylene and the second-row hydride, resulting in a smaller value for the intermediate binding energy. All together this leads to the binding energies of the germylene−Lewis basis complex as follows: NH_3 > H_2O > PH_3 > H_2S ∼ HF > HCl ≫ SiH_4 ∼ CH_4. In short, the trend

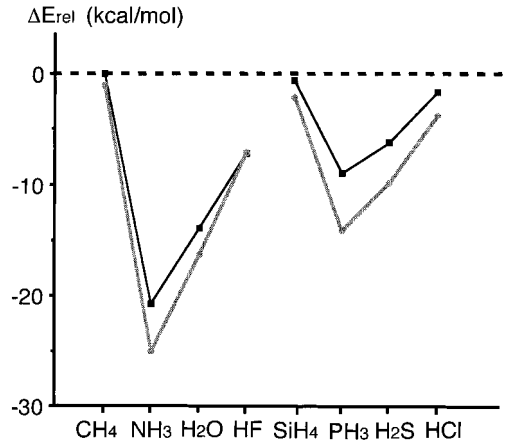

Figure 3. Binding energies of the dimethylgermylene−XH_n ($n = 1-4$) complexes calculated at the B3LYP/6-311G* and MP2/6-311G* (in a lighter line) levels of theory. The relative energies are given in Table 2.

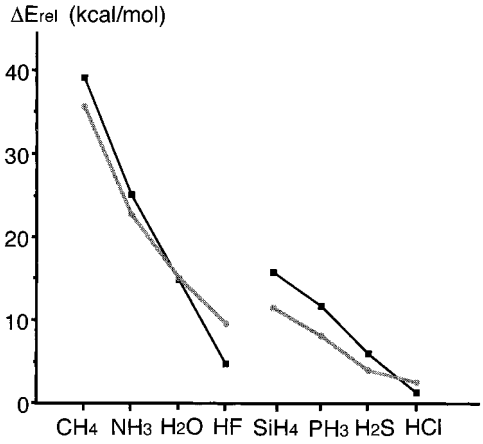

Figure 4. Activation energies for the insertion of dimethylgermylene into the X−H bond of XH_n ($n = 1-4$) molecules. All were calculated at the B3LYP/6-311G* and MP2/6-311G* (in a lighter line) levels of theory. The relative energies are given in Table 2.

in the stability of the precursor complexes can be explained by the nature of the XH_n hydride and that of germylene, and by steric effects.

The formation of complexes between germylenes and Lewis base, which strongly stabilize those divalent species, has been reported in several publications for R_2Ge- - -B (R = alkyl, aryl; B = Et_3N, PPH_3) and X_2Ge- - -B (X = F, Cl, Br; B = $C_4H_8O_2$, THF, etc.).[6,7] For instance, it has been observed that dimethylgermylenes form stable complexes with donors R_3N and R_3P at room temperature.[19] Also, there is matrix (Ar) IR evidence for the existence of complex Me_2Ge- - -OH_2 and H_2Ge- - -$^{18}OH_2$.[20] Moreover, hetero-containing substrates ROH, R_2O, R_2S, RSR′, and RCl have been shown to form adducts with dialkylgermylenes which show characteristic absorption bands at shorter wavelengths than those of the free dialkylgermylenes.[21] Many interesting examples can be found in refs 6 and 7.

B. Transition States. The results for the transition states (TS) of the germylene insertion into the H−X bonds are the most interesting results of the present study since very little was known about the barrier heights before. The optimized transition states along with the calculated transition vectors for the insertion reaction between dimethylgermylene and the XH_n molecules are given in Figures 1 and 2. The activation barriers are given in Table 2 and Figure 4.

All transition states at the B3LYP level of theory are confirmed by calculation of the energy Hessian which shows only one imaginary vibrational frequency: 1179i cm^{-1} (CH_4-TS), 1437i cm^{-1} (NH_3-TS), 1369i cm^{-1} (H_2O-TS), 1203i cm^{-1} (HF-TS), 732i cm^{-1} (SiH_4-TS), 757i cm^{-1} (PH_3-TS), 870i cm^{-1} (H_2S-TS), and 619i cm^{-1} (HCl-TS). Decomposition of the imaginary mode into internal coordinate displacements shows the major component to be X−H bond breaking, as one would expect for a true insertion TS (see Figures 1 and 2). Apparently, the transition states connect the corresponding precursor complexes to the insertion products. It should be mentioned that the primary similarity among those transition states is the three-center pattern involving germanium, hydrogen, and heteroatoms.

One of the interesting points to emerge from calculations of TS geometries is the extent to which Ge−H and Ge−X bonds are formed in the transition state. Relative to their values in the product (vide infra), the Ge−H and Ge−X bond lengths in CH_4-TS, NH_3-TS, H_2O-TS, and HF-TS are (1.0%, 9.2%), (7.3%, 10%), (6.7%, 15%), and (8.9%, 21%) longer than those in the corresponding products, respectively. Additionally, the distance of the X−H bond to be broken is 52%, 47%, 44%, and 35% longer than that of the corresponding reactant XH_n for X = C, N, O, and F, respectively. All these features indicate that the F−H and O−H insertion reactions arrive at the TS relatively early, whereas the C−H and N−H insertion reactions reach the TS relatively late. In other words, this indicates that the closer the X atom is to the end of a period, the earlier the transition state is formed. These observations will be related to the predicted energetics below.

We now consider the barriers for germylene insertion into the first- and second-row hydrides. As can be seen from Table 2 and Figure 3, the barrier heights of the transition states for germylene insertion, calculated at different levels of theory, are similar. Changes in the calculated relative energies are less than 4.8 kcal/mol from B3LYP to MP2 calculations. Furthermore, from both B3LYP and MP2 data, one may obtain two main results: (a) the activation barrier decreases in the order CH_4 > NH_3 > H_2O > HF and SiH_4 > PH_3 > H_2S > HCl, and (b) the barrier heights for the first-row hydrides are much higher than those for the second-row hydrides, i.e., CH_4 > SiH_4, NH_3 > PH_3, H_2O > H_2S, and HF > HCl. For instance, the B3LYP calculations estimate that the energies of CH_4-TS, NH_3-TS, H_2O-TS, and HF-TS are above those of the reactants by 39, 25, 15, and 4.7 kcal/mol and the activation energies from the corresponding precursor complex are 39, 46, 31, and 12 kcal/mol, respectively. Also, the DFT calculations suggest that the energies of SiH_4-TS, PH_3-TS, H_2S-TS, and HCl-TS are above those of the reactants by 16, 12, 6.0, and 1.2 kcal/mol and the activation energies for the overall reaction are 16, 21, 12, and 5.6 kcal/mol, respectively. On this basis, one may therefore conclude that the germylene insertion reaction with XH (X = F, Cl) and XH_2 (X = O, S) is essentially more favorable than that with XH_4 (X = C, Si) and XH_3 (X = N, P). In addition, the model calculations also suggest that X−H insertions for the second-row hydrides occur more readily than those for the first-row hydrides. Consequently, our theoretical results are in complete accord with the Hammond postulate,[22] which associates a reactant-like transition state with a smaller barrier and a more exothermic reaction (vide infra).

Our theoretical findings are consistent with available experimental evidence. For example, it seems to be generally agreed that C−H bonds are significantly stable toward germylenes.[7,23,24] In addition, insertion of Me_2Ge into the Si−H bond of various organosilanes has been observed.[24,25] Also, acidic N−H moieties can insert free Me_2Ge; phthalimide thus forms 1,2-$C_6H_4(CO)_2$-

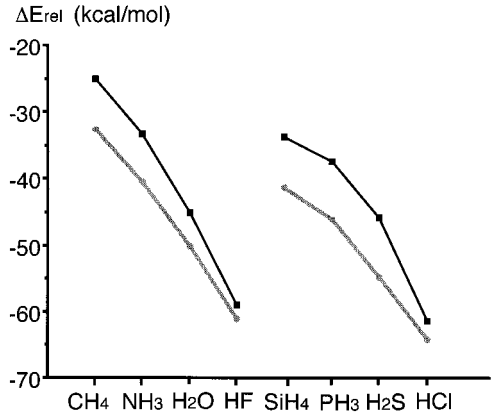

Figure 5. Energies for the $(CH_3)_2Ge(H)(XH_{n-1})$ ($n = 1-4$) insertion products calculated relative to the corresponding reactants, $Ge(CH_3)_2 + XH_n$. All were calculated at the B3LYP/6-311G* and MP2/6-311G* (in a lighter line) levels of theory. The relative energies are given in Table 2.

TABLE 3: Bond Lengths (Å) of Certain Germanium Compounds[a]

molecules	calcd[b]	expt[c]
$(CH_3)_2(H)Ge-CH_3$	1.97 (1.95)	
$(CH_3)_3Ge-CH_3$		1.98
$(CH_3)_2(H)Ge-NH_2$	1.86 (1.84)	
$H_3Ge-N(GeH_3)_2$		1.84
$(CH_3)_2(H)Ge-OH$	1.81 (1.79)	
$H_3Ge-O(GeH_3)$		1.77
$(CH_3)_2(H)Ge-F$	1.78 (1.77)	
F_3Ge-F		1.68
$(CH_3)_2(H)Ge-SiH_3$	2.40 (2.38)	
$H_3Ge-SiH_3$		2.36
$(CH_3)_2(H)Ge-PH_2$	2.36 (2.33)	
$H_3Ge-P(GeH_3)_2$		2.31
$(CH_3)_2(H)Ge-SH$	2.27 (2.24)	
$H_3Ge-S(GeH_3)$		2.20
$(CH_3)_2(H)Ge-Cl$	2.21 (2.18)	
Cl_3Ge-Cl		2.19

[a] All were calculated at the B3LYP/6-311G* and MP2/6-311G* (in parentheses) levels of theory. [b] The calculated structures can be found in Figures 1 and 2, respectively. [c] The experimental data see ref 35.

NMe_2GeH.[7] Moreover, it has been shown that free germylene Me_2Ge inserts smoothly into O−H and S−H bonds of water, deuterium oxide, and oximes.[6,7] No estimates of the activation energies of these processes are available.

C. Insertion Products. The equilibrium geometries for the insertion products (CH_4-IP, H_2O-IP, NH_3-IP, HF-IP, and SiH_4-IP, PH_3-IP, H_2S-IP, HCl-IP) are presented in Figures 1 and 2, respectively. The reaction enthalpies at both B3LYP and MP2 levels of theory are plotted in Figure 5 together with the reaction enthalpies of the XH_n hydride systems given in Table 2.

The theoretical results depicted in Figures 1 and 2 show that all the insertion products $(CH_3)_2Ge(H)(XH_{n-1})$ adopt a tetracoordinate conformation on the germanium center. Unfortunately, experimental structures for those insertion products are not known. Nevertheless, partial comparisons with experimental structures are made in Table 3 for $(CH_3)_2Ge(H)(XH_{n-1})$ compounds. From this table, it can be seen that the predicted structures may be compared qualitatively with experimental geometries of substituted analogues.

Furthermore, it is apparent that all the germylene insertions are thermodynamically exothermic. In fact, from Figure 5 it can first be noted that there are large similarities in the trends for the first-row and second-row insertion products. There is, for example, a clear trend toward larger reaction enthalpy on moving along a row. Namely, the B3LYP results suggest that the reaction enthalpy for the first-row XH_n hydrides decreases in the order CH_4-IP (−25 kcal/mol) > NH_3-IP (−33 kcal/mol) > H_2O-IP (−45 kcal/mol) > HF-IP (−59 kcal/mol). Likewise, the exothermicity for the second-row XH_n hydrides is predicted to be in the order SiH_4-IP (−34 kcal/mol) > PH_3-IP (−37 kcal/mol) > H_2S-IP (−46 kcal/mol) > HCl-IP (−56 kcal/mol). On the other hand, as shown in Table 2, the main difference between the first- and second-row X−H insertions is that the latter are more exothermic and their activation barriers lower. Again, these results are consistent with the prediction that the activation barrier should be correlated to the exothermicity for the germylene insertion.[8]

TABLE 4: Activation Energies (kcal/mol) for the Methylene, Silylene, and Dimethylgermylene Insertion Reactions

XH_n	CH_2[a]	SiH_2[b]	$Ge(CH_3)_2$[c]
$H-CH_3$	∼0	+18	+39
$H-NH_2$	∼0	+13	+25
H−OH	∼0	+9.0	+15
H−F	∼0	+3.0	+4.7
$H-SiH_3$	∼0	∼0	+16
$H-PH_2$		+2.0	+25
H−SH		+5.0	+6.0
H−Cl		+6.0	+1.2

[a] See ref 36. [b] See refs 26 and 36. [c] This work.

In summary, the periodic trends in the energetics of these eight systems are especially interesting. First, our theoretical findings indicate that for germylene insertions there is a very clear trend toward lower activation barriers and more exothermic interactions on going from left to right along a given row. Second, for the second-row hydrides, the insertion reactions are more exothermic than for the first-row hydrides and the reaction barriers are lower.

D. Comparison with Methylene and Silylene Insertions. To obtain a better understanding of the nature of the germylene insertion reaction, a comparison is made between the reaction mechanisms and energetics of the germylene insertions and those of carbene and silylene analogues. Although carbenes have long been the subject of intense experimental and theoretical investigations,[1] there is, to our knowledge, no systematic study of the reactions of carbene with a series of XH_n hydrides, and thus the detail of such carbene insertion mechanisms still is obscure.[26] Indeed, it is well-known that the reactions of carbene are of considerable complexity,[1] a variety of possible processes commonly taking place with considerable ease. This is due in part to the very great inherent reactivity of carbene, its reactions consequently having low activation energies so that the differences between different reaction pathways are very small.[27] On the other hand, the existence and the nature of silylene insertion reactions with the XH_n molecules were theoretically studied by Gordon[28] and were later confirmed by some experimental observations.[29] In spite of the fact that the available data are rather limited, several known examples (which are collected in Table 4) give us a clue to understanding the nature of divalent species insertion reactions.

Although the data in Table 4 were calculated at different levels of theory, several interesting results may be found in this table. Qualitatively, it seems to be generally accepted that insertion into O−H and N−H bonds is more favorable than insertion into C−H bonds.[1] This finding is consistent with the predictions of the germylene insertions presented in this work. Moreover, our theoretical results for the structures and the periodic trends of germylene insertion reactions are quite similar to those for the analogous silylene insertions calculated by

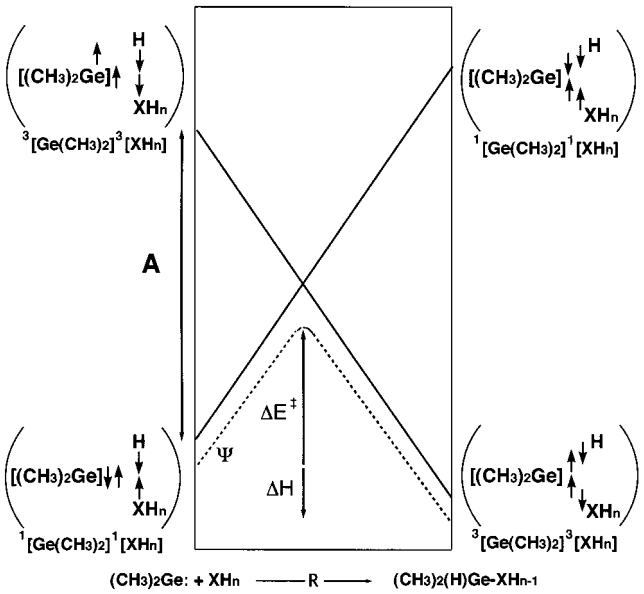

Figure 6. Energy diagram for an insertion reaction showing the formation of a state curve (Ψ) by mixing two configurations: the reactant configuration (I_R) and the product configuration (I_P). In the reactants, they are separated by an energy gap A. Configuration mixing near the crossing point causes an avoided crossing (dotted line).

Gordon.[28] For instance, the theoretical calculations show that the X−H insertion for the second-row hydrides has a lower activation barrier than that for the first-row hydrides. Furthermore, the calculations have established that carbene insertion into single σ bonds does not require the energy barrier to be overcome and proceeds as a concerted reaction without further reaction intermediates. In contrast, silylene and germylene insertions have a larger activation barrier. All these results strongly indicate that the chemical behavior of germylene is quite similar to that of silylene, but not that of carbene. The reason for this is presumably due to electronic effects. Namely, as mentioned earlier, the singlet−triplet splitting and the structure of the substituted germylenes show much greater similarities with their silicon counterparts[30] than with their carbene analogues. As we shall show below, this difference of behavior between carbene and silylene/germylene is linked to the singlet−triplet splitting of divalent species, which plays an important role in determining the activation energy of the insertion reaction.

E. The Configuration Mixing Model. All these computational results can be rationalized on the basis of a simple valence bond (VB) model based upon reactant and product spin recoupling, which is often described as the configuration mixing (CM) model.[31,32] In this approach the total energy profile is decomposed into two components, one associated with the reactant spin coupling and the other with the product spin coupling. These two component curves are denoted as reactant configuration (I_R) and product configuration (I_P), respectively.

In Figure 6, we represent the qualitative behavior of the two configurations for the germylene insertion into a X−H bond. We use I_R and I_P to denote the insertion reactant−product spin coupling. I_R describes a situation where the two electrons on the germylene are spin-paired to form the lone pair, while the two electrons on the XH_n hydride are spin-paired to form an X−H σ bond as illustrated in **2**. On the other hand, I_P corresponds to a situation where the electron pairs are coupled to allow both Ge−X and Ge−H bond formation and simultaneous X−H bond breaking. See **3**. To obtain this configuration from the reactant configuration I_R **2**, each of the two original electron pairs needs to be uncoupled, requiring the excitation of the electron pairs from the singlet state to the triplet state. Thus, I_P describes an overall singlet configuration, despite the fact that it contains two local triplets. Its valence excitation energy corresponds to the energy gap (*A*) in the CM model between the reactant (I_R) and product (I_P) configuration. The MO representations of VB configurations **2** and **3** are shown in **4** and **5**, respectively.

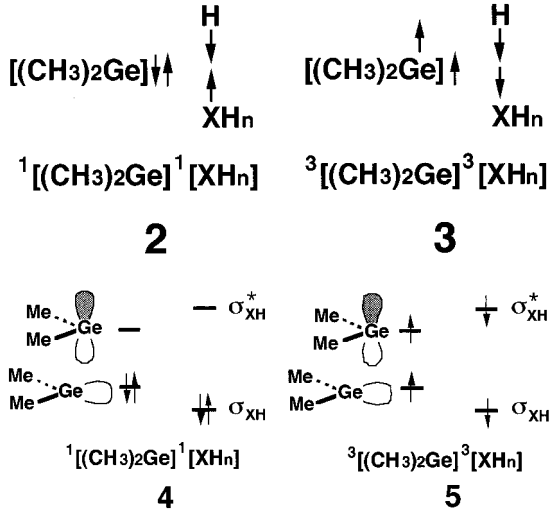

As the reaction proceeds, the energy of I_R rises and that of I_P drops. The transition state is reached at a point along the reaction coordinate where the energy curves of I_R and I_P cross. The reaction systems reaches a maximum energy somewhat below the crossing point, due to I_R-I_P configuration mixing near the transition state or, in other words, an avoided crossing; this is indicated by the dotted curves in Figure 6. Finally, in the products the roles of I_R and I_P have been inverted: I_P has become the ground-state configuration and I_R an excited state. In our example, I_P has been turned into the ground-state configuration of the insertion product $(CH_3)_2Ge(H)(XH_{n-1})$ and I_R corresponds to a doubly excited state of this compound as mentioned above. As seen in Figure 6, it is clear that both the barrier height ($\Delta E^{\ddagger}$) and the reaction enthalpy (ΔH) may be expressed in terms of the initial energy gap (*A*) between the reactant (I_R) and product (I_P) configurations. That is to say, $A = \Delta E_{\sigma\sigma^*}$ (i.e., the σ(X−H) → σ *(X−H) triplet excitation energy for XH_n) + ΔE_{st} (i.e., the germylene singlet−triplet splitting). Accordingly, if ΔE_{st} is a constant and $\Delta E_{\sigma\sigma^*}$ is reduced, then curve crossing occurs at a lower energy, leading to a lower barrier and a larger exothermicity. Bearing this CM model (Figure 6) in mind, we shall explain the origin of the observed trends as shown previously in the following discussion:

(a) Why does the ease of germylene insertion into X−H bond increase in the order C−H < N−H < O−H < F−H and Si−H < P−H < S−H < Cl−H?

Before analyzing the results, it is intriguing to note that the X−H bond strengths for the first- and second-row hydrides increase respectively in the order H−CH_3 (105 kcal/mol) < H−NH_2 (108 kcal/mol) < H−OH (119 kcal/mol) < H−F (135 kcal/mol) and H−PH_2 (83.9 kcal/mol) < H−SH (91.2 kcal/mol) < H−SiH_3 (91.8 kcal/mol) < H−Cl (103 kcal/mol).[33] However, it has been shown in this work that for germylene insertion the methane C−H bond is more difficult to activate than the ammonia N−H bond and water O−H bond, which in turn is more difficult to activate than the hydrogen fluoride F−H bond. The same situation can also be found in the second-row

hydrides as shown earlier. This cannot be explained by the initial X−H bond strength, since the X−H bond in XH_n to the right is stronger than the one to the left in the periodic table. In other words, there is a general inverse correlation between the initial X−H bond strength and the difficulty to activate this bond by germylenes.

The explanation is instead connected with electronic and steric effects. According to the CM model as discussed above, the $\Delta E_{\sigma\sigma^*}$ in the XH_n hydride should play a significant role in the insertion reactions of germylene into the X−H bonds. Namely, a smaller $\Delta E_{\sigma\sigma^*}$ in the XH_n molecule results in a lower barrier height and a larger exothermicity. Our B3LYP results suggest a decreasing trend in $\Delta E_{\sigma\sigma^*}$[34,35] for CH_4 (249 kcal/mol) > HF (227 kcal/mol) > H_2O (163 kcal/mol) > NH_3 (152 kcal/mol) and SiH_4 (205 kcal/mol) > HCl (166 kcal/mol) > PH_3 (140 kcal/mol) > H_2S (130 kcal/mol), which is in reasonable agreement with the trend in the activation energy as well as the enthalpy for $GeMe_2$ insertion as shown in Table 2. It must be emphasized here that the ordering of the X−H bond strength follows a different trend than $\Delta E_{\sigma\sigma^*}$.

Another contributing factor of major importance for the order of the barriers is the steric effect.[36] It is clear by inspection of Figure 1 that it is relatively easy for the germylene to approach the X−H (X = F, Cl) molecule and a lower barrier for this reaction than for the other XH_n hydride reactions is therefore expected. For methane and silane, on the other hand, a substantial initial distortion of the molecules is needed to reach a proper interaction; see Figures 1 and 2. For NH_3, H_2O or PH_3, H_2S, the situation is somewhat between that of XH and XH_4 molecules. Consequently, both electronic and steric effects reinforce each other to make the F−H or Cl−H insertion much more favorable than other X−H ones on both kinetic and thermodynamic grounds.

(b) Why, for the same family, is the second-row hydride XH_n generally easier and more exothermic than the first-row one in germylene insertion into the X−H bonds?

The driving force of this may also be traced to $\Delta E_{\sigma\sigma^*}$ of XH_n and its steric effect. Nevertheless, for the same family systems, the steric factor can be considered as a constant and the electronic factor may come to play a dominant role in the course of the insertion reaction of germylenes into the H−X bond of XH_n molecules. As mentioned earlier, the B3LYP calculations suggest a decreasing trend in $\Delta E_{\sigma\sigma^*}$ for CH_4 (249 kcal/mol) > SiH_4 (205 kcal/mol), NH_3 (163 kcal/mol) > PH_3 (140 kcal/mol), H_2O (152 kcal/mol) > H_2S (130 kcal/mol), and HF (227 kcal/mol) > HCl (166 kcal/mol). This correlates well with the trend of the barrier height and the exothermicity as shown previously. Again, our theoretical findings are in good agreement with the CM model.

IV. Conclusion

In the present work, we have studied the reaction mechanisms of dimethylgermylene insertion into the X−H bond of the first- and second-row XH_n molecules by both conventional ab initio method and density functional theory. In comparison with the well-defined theory (MP2/6-311G*), our model calculations have shown that the B3LYP/6-311G* level can be an alternative method to investigate the heavy atom insertion process since the B3LYP values reproduce the MP2 results very well. It should be pointed out that this study has provided the first theoretical demonstration about the reaction trajectory and theoretical estimation of the activation energy and reaction enthalpy for those processes. Moreover, we have demonstrated that the computational results can be rationalized using a simple CM model. Thus, not only have we given an explanation of some available experimental observations, but we have also made predictions for the insertion of germylene into X−H bonds.

The theoretical results suggest that a singlet germylene inserts in a concerted manner via a three-center-type transition state, and that the stereochemistry at the heteroatom X center is preserved. In addition, the order of the stability of the germylene-XH_n adduct is predicted to be $NH_3 > H_2O > PH_3 > H_2S \sim HF > HCl \gg SiH_4 \sim CH_4$.

From both a kinetic and theromodynamic viewpoint, for X−H bonds the order of reactivity by germylene insertion is Cl > F > S > O > P > N ≫ Si > C.

In other words, the greater the atomic number of heteroatom (X) in a given row, the easier the insertion reaction of XH_n hydrides and the larger the exothermicity. Moreover, the present work also shows that those results can be easily understood in terms of electronic and steric effects. Furthermore, these theoretical findings indicate that the chemical behavior of germylene should be more similar to that of silylene than to that of carbene species. Unfortunately, as we have mentioned earlier, because of a lack of experimental and theoretical data on such insertion reactions, our conclusions above may be considered as predictions for future investigations.

We thus encourage experimentalists to carry out further experiments to confirm our predictions.

Acknowledgment. We are very grateful to the National Center for High-Performance Computing of Taiwan and the Computing Center at Tsing Hua University for generous amounts of computing time. We also thank the National Science Council of Taiwan for their financial support.

References and Notes

(1) For reviews, see: (a) Hine, J. *Divalent Carbon*; Academic Press: New York, 1964. (b) Kirmse, W. *Carbene Chemistry*, 1st ed.; Academic Press: New York, 1964; Chapter 1. (c) Bethell, D. *Adv. Phys. Org. Chem.* **1969**, *7*, 153−209. (d) Moss, R. A. *Selective Organic Transformations*; Thyagarajan, B. S., Ed.; Wiley: New York, 1970; pp 35−88. (e) Krimes, W. Carbene Chemistry, 2nd ed.; Academic Press: New York, 1971; Chapter 8. (f) Moss, R. A.; Jones, M., Jr. *Carbenes*; Wiley: New York, 1973; Vol. 1. (g) Jones, M., Jr.; Moss, R. A. *Carbenes*; Wiley: New York, 1975; Vol. 2. (h) Moss, R. A.; Jones, M., Jr. *Reactive Intermediates*; Wiley: New York, 1978; Vol. 1. (i) Moss, R. A.; Jones, M., Jr. *Reactive Intermediates*; Wiley: New York, 1981; Vol. 2, Chapter 3. (j) Moss, R. A.; Jones, M., Jr. *Reactive Intermediates*; Wiley: New York, 1985; Vol. 3, Chapter 3. (k) Abramovitch, R. A. *Reactive Intermediates*; Plenum: New York, 1980; Vol. 1. (l) Platz, M. S. *Kinetics and Spectroscopy of Carbenes and Biradicals*, Plenum: New York, 1990.

(2) (a) Baldridge, K. K.; Boatz, J. A.; Koseki, S.; Gordon, M. S. *Annu. Rev. Phys. Chem.* **1987**, *38*, 211. (b) Apeloig, Y. *The Chemistry of Organic Silicon Compounds*; Patai, S., Rappoport, Z., Eds.; Wiley: Chichester, 1989. (c) Jutzi, P. *Frontiers of Organosilicon Chemistry*; Bassindale, A. R., Gaspar, P. P., Eds.; Royal Society of Chemistry: Cambridge, 1991.

(3) (a) Lesbre, M.; Mazerroles, P.; Satge, J. *The Organic Compounds of Germanium*; Zinatne: Riga, 1990. (b) Lukevics, E.; Gar, T.; Ignatovich, L.; Mironov, B. *Biological Activity of Germanium*; Zinatne: Riga, 1993. (c) Lukevics, E.; Ignatovich, L. *Frontiers of Organogermanium−Tin−Lead Chemistry*; Latvian Institute: Riga, 1993. (d) Patai, S. *The Chemistry of Organic Germanium, Tin, and Lead Compounds*; Wiley: 1995.

(4) Stabilization of germylenes can be achieved by n-donor or p-donor substituents, which reduce the electrophilicity of the germanium atom donating electrons into its vacant p-orbital, and by bulky substituents to prevent dimerization or oligomerization. See: Winter, J. G.; Portius, P.; Kociok-Kohn, G.; Steck, R.; Filippou, A. C. *Organometallics* **1998**, *17*, 4176, and references therein.

(5) For theoretical investigations concerning the addition chemistry of germylene, see: Su, M.-D.; Chu, S.-Y. *J. Am. Chem. Soc.*, in print.

(6) Riviere, P.; Riviere-Baudet, M.; Satge, J. In *Comprehensive Organometallic Chemistry*; Abel, E. W., Stone, F. G. A., Wilkinson, G., Eds.; Pergamon: Oxford, U.K., 1995; Vol. 2, pp 193.

(7) Neumann, W. P. *Chem. Rev.* **1991**, *91*, 311, and references therein.

(8) (a) Su, M.-D.; Chu, S.-Y. *J. Am. Chem. Soc.* **1999**, *121*, 4229. (b) Su, M.-D.; Chu, S.-Y. *Tetrahedron Lett.* **1999**, *40*, 4371.

(9) (a) Becke, A. D. *Phys. Rev. A* **1988**, *38*, 3098. (b) Lee, C.; Yang, W.; Parr, R. G. *Phys. Rev. B* **1988**, *37*, 785.

(10) Becke, A. D. *J. Chem. Phys.* **1993**, *98*, 5648.

(11) Ricca, A.; Bauschlicher, C. W. *Theor. Chim. Acta* **1995**, *92*, 123.

(12) (a) Krishnan, R.; Binkley, J. S.; Seeger, R.; Pople, J. A. *J. Chem. Phys.* **1980**, *72*, 650. (b) Curtiss, L. A.; McGrath, M. P.; Blaudeau, J.-P.; Davis, N. E.; Binning, R. C.; Radom, L. *J. Chem. Phys.* **1995**, *103*, 6104.

(13) Frisch, M. J.; Pople, J. A.; Binkley, J. S. *J. Chem. Phys.* **1984**, *80*, 3265.

(14) Møller, C.; Plesset, M. S. *Phys. Rev.* **1934**, *46*, 618.

(15) Frisch, M. J.; Trucks, G. W.; Schlegel, H. B.; Gill, P. M. W.; Johnson, B. G.; Robb, M. A.; Cheeseman, J. R.; Keith, T.; Peterson, G. A.; Montgomery, J. A.; Raghavachari, K.; Al-Laham, M. A.; Zakrzewski, V. G.; Ortiz, J. V.; Foresman, J. B.; Cioslowski, J.; Stefanov, B. B.; Nanayakara, A.; Challacombe, M.; Peng, C. Y.; Ayala, P. Y.; Chen, W.; Wong, M. W.; Andres, J. L.; Replogle, E. S.; Gomperts, R.; Martin, R. L.; Fox, D. J.; Binkley, J. S.; Defrees, D. J.; Baker, J.; Stewart, J. P.; Head-Gordon, M.; Gonzalez, C.; Pople, J. A.; *Gaussian 94*; Gaussian, Inc.: Pittsburgh, PA, 1995.

(16) (a) Cramer, C. J.; Dulles, F. J.; Storer, J. W.; Worthington, S. E. *Chem. Phys. Lett.* **1994**, *218*, 387. (b) For the experimental evidence see: Kocher, J.; Lehnig, M. *Organometallics* **1984**, *3*, 937.

(17) (a) For $C(CH_3)_2$ see: Richards, C. A.; Kim, S.-J.; Yamaguchi, Y.; Schaefer, H. F. III. *J. Am. Chem. Soc.* **1995**, *117*, 10104. (b) For $Si(CH_3)_2$ see: Krogh-Jespersen, K. *J. Am. Chem. Soc.* **1985**, *107*, 537. (c) For $Ge(CH_3)_2$ see: Shusterman, A. J.; Landrum, B. E.; Miller, R. L. *Organometallics* **1989**, *8*, 1851.

(18) Isaacs, N. S. *Physical Organic Chemistry*; Wiley: New York, 1995; p 199.

(19) Barrau, J.; Bouchaut, M.; Lavayssieve, H.; Dousse, G.; Satge, J. *J. Organomet. Chem.* **1983**, *243*, 281.

(20) (a) Withnall, R.; Andrews, L. *J. Phys. Chem.* **1990**, *94*, 2351. (b) Nowek, A.; Leszczynski, J. *J. Phys. Chem. A* **1997**, *101*, 3784.

(21) Ando, W.; Itoh, H.; Tsumuraya, T. *Organometallics* **1989**, *8*, 2759.

(22) Hammond, G. S. *J. Am. Chem. Soc.* **1954**, *77*, 334.

(23) (a) Lange, L.; Meyer, B.; DuMont, W.-W. *J. Organomet. Chem.* **1987**, *329*, C17. After this paper was submitted, four recent papers related germylene insertions into C−H bonds have been found: (b) Jutzi, P.; Schmidt, H.; Neumann, B.; Stammler, H.-G., Organometallics, **1996**, *15*, 741. (c) Lei, D.; Lee, M. E.; Gaspar, P. P.; Tetrahedron, **1997**, *53*, 10179. (d) Becerra, R.; Boganov, S. E.; Egorov, M. P.; Lee, V. Y.; Nefedov, O. M.; Walsh, R. *Chem. Phys. Lett.* **1996**, *250*, 111. (e) Becerra, R.; Boganov, S. E.; Egorov, M. P.; Faustov, V. I.; Nefedov, O. M.; Walsh, R. *J. Am. Chem. Soc.* **1998**, *120*, 12657.

(24) (a) Becerra, R.; Boganov, S. E.; Egorov, M. P.; Nefedov, O. M.; Walsh, R. *Chem. Phys. Lett.* **1996**, *260*, 433. (b) Becerra, R.; Boganov, S. E.; Egorov, M. P.; Faustov, V. I.; Nefedov, O. M.; Walsh, R. *J. Am. Chem. Soc.* **1998**, *120*, 12657.

(25) (a) Mochida, K.; Hasegawa, A. *Chem. Lett.* **1989**, 1087. (b) Baines, K. M.; Cooke, J. A. *Organometallics* **1992**, *11*, 3487. (c) Baines, K. M.; Cooke, J. A.; Vittal, J. J. *J. Chem. Soc., Chem. Commun.* **1992**, 1484.

(26) Bach, R. D.; Andres, J. L.; Su, M.-D.; McDouall, J. J. W. *J. Am. Chem. Soc.* **1993**, *115*, 5768.

(27) For instance, there are several possible mechanisms for the O−H insertion reaction of carbene. See: Krimse, W.; Meinert, T.; Modarelli, D. A.; Platz, M. S. *J. Am. Chem. Soc.* **1993**, *115*, 8918.

(28) Raghavachari, K.; Chandrasekhar, J.; Gordon, M. S.; Dykenma, K. J. *J. Am. Chem. Soc.* **1984**, *106*, 5853.

(29) (a) Gillette, G. R.; Noren, G. H.; West, R. *Organometallics* **1989**, *8*, 487. (b) Ando, W.; Sekiguchi, A.; Hagiwara, K., Sakakibara, A.; Yoshida, H. *Organometallics* **1988**, *7*, 558.

(30) Pettersson, L. G. M.; Schule, J. *J. Mol. Struct.* **1990**, *208*, 137.

(31) (a) Shaik, S.; Schlegel, H. B.; Wolfe, S. *Theoretical Aspects of Physical Organic Chemistry*; John Wiley & Sons Inc.: New York, 1992. (b) Pross, A. *Theoretical and Physical Principles of Organic Reactivity*; John Wiley & Sons Inc.: New York, 1995.

(32) Su, M.-D. *Inorg. Chem.* **1995**, *34*, 3829.

(33) Kerr, J. A. *CRC Handbook of Chemistry and Physics*, 75th ed.; West, R. C., Ed.; CRC: Boca Raton, NY, 1988.

(34) $\Delta E_{\sigma\sigma^*}$ can be evaluated to a good approximation from the energies of the vertical $\sigma(X-H) \rightarrow \sigma^*(X-H)$ triplet excitation in the XH_n hydrides, in which the triplet state was calculated at B3LYP/6-311G* using the singlet geometry of the same level. For details see ref 33.

(35) Su, M.-D.; Chu, S.-Y. *Eur. J. Chem.* **1999**, *5*, 198.

(36) Similar steric arguments have been successful in explaining the trend in activation barriers for H−H, C−H, and C−C bond breaking reactions by transition metal complexes and can also be used to explain the lower barrier for the C−H bond breaking in various kinds of hydrocarbons. See: Siegbahn, P. E. M.; Blomberg, M. R. A. *Theoretical Aspects of Homogeneous Catalysis*; van Leeuwen, P. W. N. M., Morokuma, K., van Lenthe, J. H., Eds.; Kluwer Academic Publishers: Dordrecht, 1995, and references therein.

(37) Riviere, P.; Riviere-Baudet, M.; Satge, J. In *Comprehensive Organometallic Chemistry*; Wilkinson, G., Stone, F. G. A., Abel, E. W., Eds.; Pergamon: Oxford, U.K., 1982; Vol. 2, Chapter 10.

(38) Minkin, V. I.; Simkin, B. Y.; Glukhovtsev, M. N. *Russ. Chem. Rev.* **1989**, *58*, 622.